ADVANCING EARTH AND SPACE SCIENCES

Geophysical Research Letters

RESEARCH LETTER
10.1029/2024GL108324

Detrital Input Sustains Diatom Production off a Glaciated Arctic Coast

Hong Chin Ng[1], Katharine R. Hendry[1,2], Rachael Ward[1], E. M. S. Woodward[3], Melanie J. Leng[4], Rebecca A. Pickering[5], and Jeffrey W. Krause[6,7]

[1]School of Earth Sciences, Wills Memorial Building, University of Bristol, Bristol, UK, [2]Polar Oceans Team, British Antarctic Survey, Cambridge, UK, [3]Plymouth Marine Laboratory, Plymouth, UK, [4]Centre for Environmental Geochemistry, School of Biosciences, Sutton Bonington Campus, University of Nottingham, Loughborough, UK, [5]Department of Geology, Lund University, Lund, Sweden, [6]Dauphin Island Sea Lab, Dauphin Island, AL, USA, [7]School of Marine and Environmental Sciences, University of South Alabama, Mobile, AL, USA

Key Points:

- Some of the highest levels of detrital amorphous silica in the Arctic Ocean are found off a glaciated Greenland coast
- Enhanced Arctic diatom production is found where detrital amorphous silica level is high, even when there is limited dissolved nutrient
- Gradual dissolution of detrital amorphous silica is estimated to sustain about half of diatom production off southwest Greenland coast

Supporting Information:

Supporting Information may be found in the online version of this article.

Correspondence to:

H. C. Ng,
hn9381@bristol.ac.uk

Citation:

Ng, H. C., Hendry, K. R., Ward, R., Woodward, E. M. S., Leng, M. J., Pickering, R. A., & Krause, J. W. (2024). Detrital input sustains diatom production off a glaciated Arctic coast. *Geophysical Research Letters*, *51*, e2024GL108324. https://doi.org/10.1029/2024GL108324

Received 21 JAN 2024
Accepted 23 MAY 2024

Author Contributions:

Conceptualization: Katharine R. Hendry
Data curation: Hong Chin Ng
Formal analysis: Hong Chin Ng, Katharine R. Hendry, Jeffrey W. Krause
Funding acquisition: Katharine R. Hendry
Investigation: Hong Chin Ng, Rachael Ward, E. M. S. Woodward, Melanie J. Leng, Rebecca A. Pickering
Methodology: Hong Chin Ng, Katharine R. Hendry, E. M. S. Woodward, Melanie J. Leng, Jeffrey W. Krause
Resources: Katharine R. Hendry, E. M. S. Woodward, Melanie J. Leng, Jeffrey W. Krause
Supervision: Katharine R. Hendry

Abstract

In the Arctic and subarctic oceans, the relatively low supply of silicon (compared to other nutrients) can make it limiting for the growth of diatoms, a fundamental building block of the oceanic food web. Glaciers release large quantities of dissolved silicon and dissolvable solid amorphous silica phases into high-latitude estuaries (fjords), but the role of these glacially-derived silica phases in sustaining diatom growth in the coastal and open-water sectors remains unknown. Here we show how stable and radiogenic silicon isotopes can be used together to address this question, using southwest Greenland as a case study. This study finds enhanced levels of detrital (i.e., mineral) amorphous silica, likely glacially-sourced, sustaining a large portion of diatom growth observed off the coast, revealing how the phytoplankton community can function during high-meltwater periods.

Plain Language Summary

Through physical grinding and chemical reactions, glaciers release a large amount of nutrients, such as silicon, from the underlying rocks. The silicon released are present in two main forms: (a) silicon dissolved in seawater, and (b) soluble silicon in glacial debris. However, there has been an ongoing debate about the contribution of this glacier-sourced nutrient to the coastal ecosystem in the high latitudes. This is because dissolved silicon concentrations in seawater have been found at low levels in glaciated fjords and coastal environments, and the offshore transportation pathways for reactive glacial debris are poorly understood. This study aims to address these outstanding questions by employing a suite of chemical and oceanographic analyses, using southwest Greenland as a case study. We find enhanced growth of a major microalgae group at sites with high glacial debris level off the coast. Our study supports the role of glacier-sourced nutrient in sustaining high-latitudinal coastal ecosystem through gradual dissolution of glacial debris, especially in regions with low levels of dissolved nutrient.

1. Introduction

The Arctic and subarctic regions are experiencing some of the most rapid environmental responses to increasing atmospheric and ocean temperatures that have been observed globally (Meredith et al., 2019). For example, increasing air temperatures are resulting in accelerated mass loss from the Greenland Ice Sheet (GrIS) via surface melting and the ice retreat at glacier fronts, potentially enhanced by warming fjord temperatures and changes in ocean circulation (Enderlin et al., 2014; Felikson et al., 2017; Shepherd et al., 2020; van den Broeke et al., 2017). Meltwater from the GrIS has the potential to impact downstream biological productivity, carbon uptake and ecosystem structure through physical changes to the water column and the supply of organic matter and inorganic nutrients to the photic zone (Meire et al., 2017; Oliver et al., 2018). These meltwaters have also been associated with offshore summertime phytoplankton blooms (Arrigo et al., 2017). Specifically, subglacial-routed meltwaters are known to be rich in several key macro- and micronutrients, including the dissolved silicon or silicic acid (DSi) (Meire et al., 2016), reactive amorphous solid phases of silica (ASi) (Hawkings et al., 2017), and iron (Fe) (Bhatia et al., 2013; Hawkings et al., 2014). A significant proportion of these dissolved inorganic nutrients are trapped within fjords by biological utilization (Hopwood et al., 2015, 2020) and abiotic processes such as adsorption and precipitation (Ng et al., 2022). Despite these consumption processes, fjord mouth waters have high concentrations of dissolved micronutrients (e.g., Fe) relative to coastal and open ocean waters (Tonnard et al., 2020). Furthermore, particulate material transported from fjords into the coastal environment (Hendry et al., 2019, 2021) will

Validation: Hong Chin Ng, Rachael Ward, E. M. S. Woodward, Melanie J. Leng, Rebecca A. Pickering
Visualization: Hong Chin Ng, Jeffrey W. Krause
Writing – original draft: Hong Chin Ng, Katharine R. Hendry, E. M. S. Woodward, Rebecca A. Pickering, Jeffrey W. Krause
Writing – review & editing: Hong Chin Ng, Katharine R. Hendry, Rebecca A. Pickering, Jeffrey W. Krause

undergo some degree of nutrient release by dissolution or desorption in the water column or shallow sediments (Hatton et al., 2023; Koziorowska et al., 2018; Laufer-Meiser et al., 2021; Ng et al., 2020), and such material may also affect biological processes.

Diatoms are a major phytoplankton group responsible for nearly half of the oceanic primary production and uptake of CO_2 (Nelson et al., 1995). They are also a fundamental building block of the oceanic food web. Notably, Arctic Ocean phytoplankton primary production has increased by 57% between 1998 and 2018 and nutrient availability is expected to be a major control of any further increase in future production (Lewis et al., 2020). Due to diatoms' obligate silicon (Si) requirement, limitation by the availability of nutrient Si in the (sub)Arctic Ocean can affect diatom processes (Giesbrecht & Varela, 2021; Krause et al., 2018, 2019). Nutrient uptake kinetic experiments have shown that diatom growth is limited in Arctic waters with DSi concentrations or [DSi] below ~2–8 μM (Giesbrecht & Varela, 2021; Krause et al., 2018), depending on the adaptation of the diatom species assemblages to the ambient nutrient conditions (Giesbrecht & Varela, 2021). Diatoms can adapt to low [DSi], for example, down to ~1 μM, by reducing the amount of biogenic silica (BSi) precipitated (silicification) when building their cell wall, such that division rates of diatom cells can remain high (despite limitation to their rate of DSi uptake) and the population size can be maintained (McNair et al., 2018). However, Arctic seawater [DSi] can drop to <0.5 μM on a seasonal timescale (Figure 1a) and such low DSi exceeds the capacity of diatoms to alter their physiology, therefore, DSi uptake limitation can transition to growth limitation by suboptimal [DSi]. This growth limitation leads to reductions in diatom biomass, and subsequent changes to phytoplankton community structure and overall primary production (Krause et al., 2019).

Despite the large amounts of DSi and dissolvable ASi exported from the GrIS (Hawkings et al., 2017), the extent to which these glacially-derived bioavailable Si phases influence surface ocean [DSi] and diatom growth in the wider (sub) Arctic Ocean remains unknown. Given that the spring diatom bloom can terminate due to DSi limitation (Krause et al., 2019), GrIS-derived bioavailable Si has the potential to modify bloom dynamics if it can relieve seasonal diatom limitation. We address these outstanding questions by employing a suite of chemical and oceanographic analyses, using southwest Greenland as a case study. In particular, stable (Debyser et al., 2022; Giesbrecht et al., 2022; Laukert et al., 2022) and radiogenic (Giesbrecht & Varela, 2021; Krause et al., 2018) Si isotopes were utilized to examine the supply and utilization of this nutrient. Our findings provide a quantitative, mechanistic understanding of the supply of glacier-sourced bioavailable Si to the surface waters of the Arctic coastal and continental shelf domain, and its role in sustaining diatom production. Such understanding is critical for deconvolving the drivers that govern the biogeochemical cycling, phytoplankton community structure, and primary production in the Arctic and subarctic ocean, which will enable robust predictions of future ecosystem changes in this climate-sensitive region.

2. Materials and Methods

2.1. Sampling Sites

Samples and oceanographic measurements were collected from three main areas: offshore from Nuuk on the southwest Greenland margin, near Narsaq and Cape Farewell on the south Greenland margin, and the Labrador Sea (Figure S1 in Supporting Information S1). There is a north-south divide in ocean water masses along the southwest Greenland slope, with waters to the south originating in the East Greenland Current (EGC), which flows around Cape Farewell, mixing with Atlantic-sourced waters to form the West Greenland Current (WGC). The WGC flows up the southwest coast of Greenland, receiving GrIS meltwater discharge and terrestrial inputs along its flow path (Hendry et al., 2019). Runoff from the GrIS enters the Labrador Sea via anticyclonic warm-core rings that are shed off the WGC near the northern part of our study area (~65°N; Rysgaard et al., 2020).

Along most of the WGC, the surface waters are characterized by low macronutrient concentrations in the top 50 m (Hendry et al., 2019). In contrast, concentrations of the key micronutrients, such as [dFe] are relatively high, particularly in the surface waters of the continental shelf and slope, corresponding to high meteoric water inputs (Tonnard et al., 2020). These nutrient observations have been linked with elevated chlorophyll *a* (Chl *a*) concentrations (Tonnard et al., 2020), which are consistent with strong biological uptake and the utilization of macronutrients (to produce Chl *a*). Despite low [DSi] and low temperatures, there is a surprisingly active diatom community along the southwest Greenland margin (Hendry et al., 2019). For example, offshore from Nuuk, the phytoplankton community is dominated (60%–100%) by diatoms (Arendt et al., 2010).

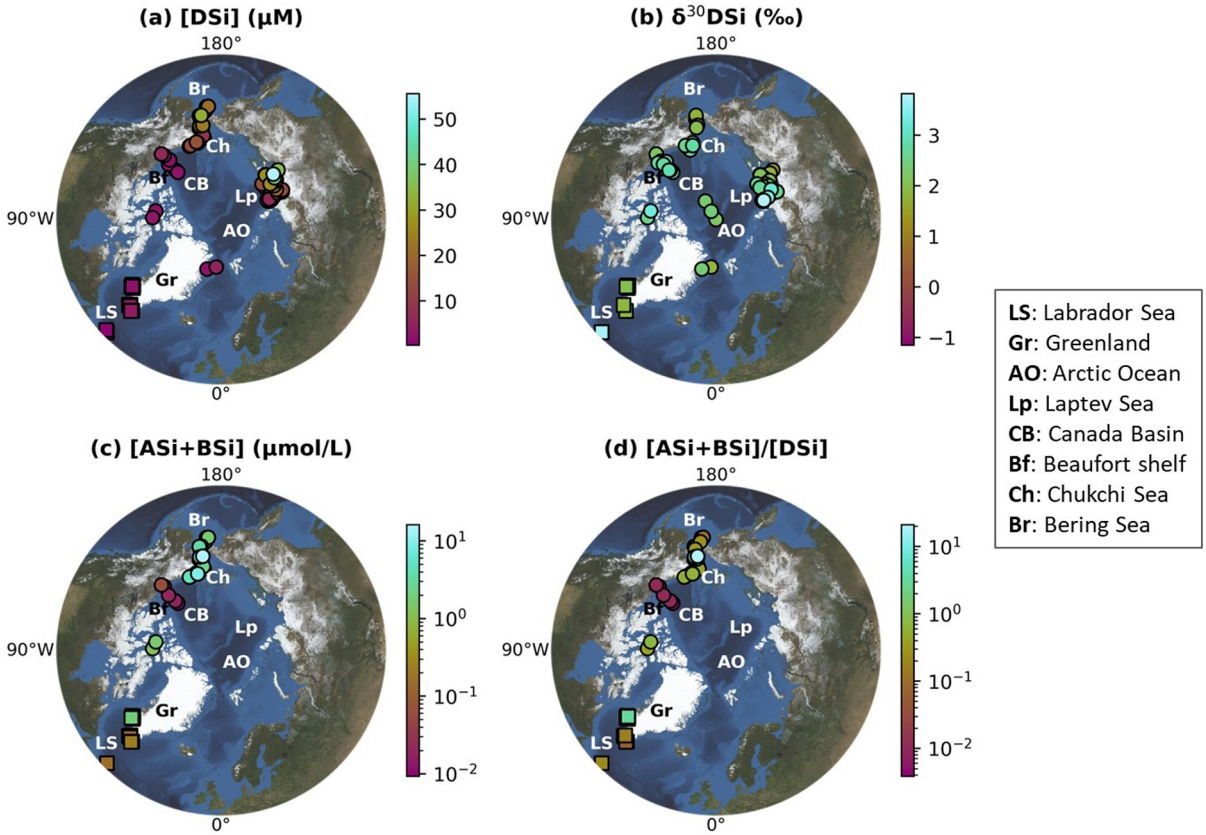

Figure 1. Maps of Arctic surface-water Si data compilation. (a) [DSi], (b) δ^{30}DSi, (c) [ASi + BSi], and (d) [ASi + BSi]/[DSi]. Results from this study are compiled with previously published data sets (Table S1 in Supporting Information S1). Values shown are summertime (July–September) data averaged over the top 10 m, which are the average mixed layer depth of the Arctic Ocean for the season. The Arctic maps (50°N–90°N, orthographic projection) were drawn using Python 3.9.7 with the Cartopy and Matplotlib packages.

2.2. Field Methodology

Hydrographic and water samples were collected on board the *RRS Discovery* from July–August 2017 (expedition DY081) (Hendry et al., 2019). Hydrographic data were obtained from a Sea-Bird SBE 9plus Conductivity Temperature Depth (CTD) unit including a WET Labs C-Star transmissometer, a Chelsea Technologies Group Aquatracka MKIII fluorometer, and a Biospherical QCP Cosine Photosynthetic Active Radiation (PAR) meter. These instruments were attached to a standard stainless steel CTD rosette which housed 24 Niskin bottles. The mixed layer depth (MLD) was defined as the depth of the maximum buoyancy frequency and was comparable to common-used density gradient metrics of MLD (Carvalho et al., 2017) (Figure S2 in Supporting Information S1). Following the GO-SHIP procedures in Hydes et al. (2010), water samples for macronutrient analysis were filtered immediately after Niskin bottle collection through 0.2 μm Acropak filters into pre-acid cleaned high density polyethylene bottles and were frozen for storage and transport to land. Prior to analysis at Plymouth Marine Laboratory, macronutrient samples were thawed following GO-SHIP nutrient protocols (Becker et al., 2020) in a warm water bath for 45 min, followed by equilibration to room temperature for a further 45 min. Samples for stable Si isotope analysis were similarly filtered but stored at ambient temperature without freezing, following GEOTRACES protocol (Sutton et al., 2018). Seawater oxygen isotopes were used together with bottle salinity measurements to deconvolve the different freshwater inputs from meteoric water (largely glacial meltwater, mixed with snow melt and non-glacial stream water in this region; Hatton et al., 2023; hereafter known as modified meltwater) and sea ice melt using mass balance calculations. Details of this salinity calibration, seawater oxygen isotope analysis, and mass balance calculations have previously been reported (Hendry et al., 2019). Suspended particulate matter was collected by filtering a known volume of seawater through polycarbonate filters (0.45 μm) which were then dried and stored at 4°C until analysis.

Diatom BSi production, measured as the rate of diatom uptake of nutrient Si, was quantified using additions of the radioisotope ^{32}Si (Krause et al., 2018). Briefly, samples were collected within the euphotic zone (the bottom of the euphotic zone was defined as 1% irradiance relative to that just below the surface) and spiked with 333 Bq of ^{32}Si (in the form of silicic acid), before being incubated in surface seawater cooled flow-through incubators on deck, to regulate temperature. A second set of euphotic zone samples were collected, enriched with DSi (+20 μM) to saturate Si uptake, and then spiked with ^{32}Si before incubations. Light levels at the depth of collection were mimicked during incubations by covering the samples with variable neutral density screening to imitate irradiance levels. The samples were filtered after incubation (1.2 μm polycarbonate membranes), and particulate ^{32}Si activity was quantified using a GM-25 Multicounter (Risø DTU National Laboratory, Denmark) after the samples had aged into secular equilibrium with ^{32}P. Diatom BSi production was determined from the ^{32}Si uptake over the incubation period (Krause et al., 2011; Supporting Information S1—Evaluating BSi production). To account for all euphotic-zone diatom BSi production at a station, rates were integrated from the surface to the base of the euphotic zone; this was done for both the ambient DSi and the enriched DSi treatments. An assessment of nutrient DSi limitation of diatom growth can be provided by the percentage ratio of diatom BSi production at ambient condition to diatom BSi production at DSi-enhanced (+20 μM) condition, $\int\rho_{ambient}/\int\rho_{enhanced}$, where values lower than 100% indicate nutrient DSi limitation (i.e., the rate of Si uptake at ambient DSi is lower than when DSi is non-limiting, presumably +20 μM).

2.3. Laboratory Methodology

The macronutrients (DSi) were analyzed using techniques as described in Woodward and Rees (2001), using a SEAL AA3 segmented-flow autoanalyzer. Data quality was ensured using certified nutrient reference materials (KANSO Ltd. Japan). The typical uncertainty of the measurements was between 2% and 3%, and the limits of detection for NO_3 and PO_4 were 0.02 μM. Water-column DSi concentrations did not ever approach the limits of detection (0.02 μM).

The ASi and BSi fractions of the suspended particulate matter were extracted using the standard sequential leaching technique, with 0.2 M NaOH set at 85°C, and leachates taken every hour for 3 hr (Lam et al., 2015). The concentrations of the extracted ASi + BSi were quantified using standard silicomolybdate chemistry (DeMaster, 1981) and measured on a VMR V-1200 spectrophotometer. Reproducibility of sample ASi + BSi content was based on measurements of duplicate samples, and was typically between 5% and 25%.

Dissolved stable silicon isotopes ($\delta^{30}DSi$) were measured at the Bristol Isotope Group laboratories, University of Bristol. Given the low [DSi] and salt-water matrix, samples were pre-concentrated using Mg-induced co-precipitation (de Souza et al., 2012) prior to purification with cation exchange resin (Biorad AG 50 W-X12) (Georg et al., 2006). Specifically, Si in the samples was co-precipitated with $Mg(OH)_2$ with 1 M NaOH (Titripur® Reag. Ph Eur grade), rinsed three times with 0.001 M NaOH, and redissolved with HCl (lab distilled), before the samples were loaded onto chromatography columns. The yields of the co-precipitation method were >95%, and had no correlation with the $\delta^{30}Si$ measurements. Samples were analyzed using a Thermo Scientific™ Neptune multi-collector inductively coupled plasma mass spectrometer (MC-ICP-MS), using a dry plasma introduction system (Apex-IR). Standard-sample bracketing (with NBS-28, NIST RM8546), intensity-matched Mg doping and H_2SO_4 doping were used to correct for internal mass bias and anionic matrix mass bias (Georg et al., 2006; Hughes et al., 2011). Samples were measured in duplicates or triplicates, where sample volume allowed, with 2 S. D. ranging from <0.01‰ to 0.27‰. The $\delta^{30}Si$ of reference standards were analyzed alongside samples to assess long-term reproducibility. Average measurements of diatomite, LMG-08 (sponge), and ALOHA1000 (Pacific seawater from 1,000 m) are +1.23 ± 0.11‰ (n = 64), −3.47 ± 0.12‰ (n = 26), and +1.24 ± 0.14‰ (n = 52) respectively, which agree with published values (Grasse et al., 2017; Hendry & Robinson, 2012; Reynolds et al., 2007). Note that the consensual $\delta^{30}Si$ value for ALOHA300 (Pacific seawater from 300 m) has a greater uncertainty and is less well-constrained than that of ALOHA1000 (Grasse et al., 2017), and so is not included as a reference material in this study. New seawater $\delta^{30}DSi$ measurements from our open ocean station (CTD1, Orphan Knoll, Labrador Sea) are within the range of previously published values from the nearest GEOTRACES stations within the open ocean of the Labrador Sea (de Souza et al., 2012; Giesbrecht et al., 2022; Sutton et al., 2018) (Figure S3 in Supporting Information S1). The $\delta^{29}Si$ and $\delta^{30}Si$ values of all standards and samples measured during this study plot on a straight line with a gradient of 0.5087 ± 0.0020, which lies within the error of kinetic (0.5105) mass-dependent fractionation (Cardinal et al., 2003). There is also no correlation between the measured

δ^{30}Si values with mass dependence difference, Mg and blank correction, Mg intensity matching, and Si intensity matching, all of which have R^2 of ≤0.01 and p of >0.1.

3. Results

The surface waters from south-west Greenland margin and the Labrador Sea have [DSi] ranging from 0.46 to 3.8 μM. These values are some of the lowest [DSi] observed around the Arctic Ocean (Figure 1a). Meanwhile, there is a large regional difference in total concentrations of Si in the reactive particulate silica phases: abiogenic ASi and diatom BSi (hereafter [ASi + BSi]) among the study sites. Off Nuuk, surface water [ASi + BSi] range up to 2.0 μmol/L (Figure 1c), while concentrations at greater depths range up to 4.7 μmol/L. In contrast, [ASi + BSi] observed for the rest of the study area are less than 0.32 μmol/L.

The coastal stations exhibit a wide range of δ^{30}DSi, from +0.9‰ to +2.3‰, with one sample measuring −1.15‰ (Supporting Information S1—Isotopic compositions of low DSi waters). Above 1 μM [DSi], there is a negative relationship between [DSi] and δ^{30}DSi; however, in very low nutrient shallow waters ([DSi] <1 μM) this relationship reverses and weakens (Figure 2a). There is a positive relationship between δ^{30}DSi and the fraction of meteoric modified meltwater present, and turbidity, although the relationship weakens in waters with lower [DSi] (Figures 2b and 2c). Meanwhile, our open ocean station in the Labrador Sea shows a steeper negative relationship between [DSi] and δ^{30}DSi, with δ^{30}DSi ranging from +1.5‰ to +3.7‰ (Figure 2a).

The measured summertime diatom BSi production integrated over the euphotic zone (at ambient condition, $\int\rho_{ambient}$) ranges from ~0.02 to 14.4 mmol/m^2/day. The highest $\int\rho_{ambient}$ is observed on the southwest Greenland margin off Nuuk (Figure 3a). The southwest Greenland $\int\rho_{ambient}$ are substantially higher than the $\int\rho_{ambient}$ observed at another Arctic site: Svalbard region (0.27–1.46 mmol/m^2/day), where the surface seawater [DSi] are similarly low (0.26–4.5 μM) (Krause et al., 2018). In contrast, our $\int\rho_{ambient}$ measurements are relatively modest when compared to the $\int\rho_{ambient}$ observed at the Bering and Chukchi Seas (0.66–62.9 mmol/m^2/day) (Giesbrecht & Varela, 2021), where the surface seawater [DSi] are significantly higher (up to 27 μM) than those at our sites (Figure 1a).

Average $\int\rho_{ambient}/\int\rho_{enhanced}$ on the southwest Greenland margin off Nuuk is 58 ± 6%, which is substantially lower than the average $\int\rho_{ambient}/\int\rho_{enhanced}$ on the south Greenland margin off Narsaq/Cape Farewell: 91 ± 9%, and those in the Labrador Sea: 86 ± 7% (Figure 3b). These results mean that diatoms in the euphotic zone off Nuuk were taking up DSi at only 58% of their maximum uptake rate, indicating a degree of kinetic limitation, but not likely growth limitation (see discussion in Krause et al. (2018)). Furthermore, there was very little quantifiable limitation at Narsaq/Cape Farewell (ratio nearly ~100%), and minor limitation in the Labrador Sea.

4. Discussion and Conclusions

The southwest Greenland margin stations off Nuuk have the highest [ASi + BSi] (Figure 1b), the highest diatom production (see Results), and some of the lowest δ^{30}DSi (Figure 2a) among the Arctic sites that have low surface seawater [DSi] (<8 μM, Figure 1a). Below we discuss how glacial detritus could provide an explanation for the observations above.

4.1. Detrital ASi on Southwest Greenland Margin

Excluding the low [DSi] seawater samples (<1 μM) that are potentially influenced by small amounts of DSi derived from organic complexation and reactive metal phases (Supporting Information S1t—Isotopic compositions of low DSi waters), the [DSi]–δ^{30}DSi trends of the southwest Greenland margin are consistent with biological utilization and isotopic fractionation in waters. We have applied a biological fractionation model (Varela et al., 2004) to our data (Supporting Information S1—Calculation of apparent isotopic fractionation), assuming that diatoms are sourcing DSi from below the MLD. This simple model reveals an overall fractionation (ε) value of −0.22 ± 0.06‰ (R^2 = 0.52, p < 0.01) for an isotopically closed system (Figure S4a in Supporting Information S1), and ε of −0.64 ± 0.16‰ (R^2 = 0.56, p < 0.01) for an isotopically open system (Figure S4b in Supporting Information S1). These apparent fractionation factors are lower than the other Arctic sites—in particular, the ε estimated at the Fram Strait, situated upstream of our study area, are −0.6‰ for a closed system and −1.1‰ for an open system (Debyser et al., 2022). The lower apparent fractionation factors observed on the southwest Greenland margin reflect the low δ^{30}DSi in the near-surface water samples with [DSi] ranging from

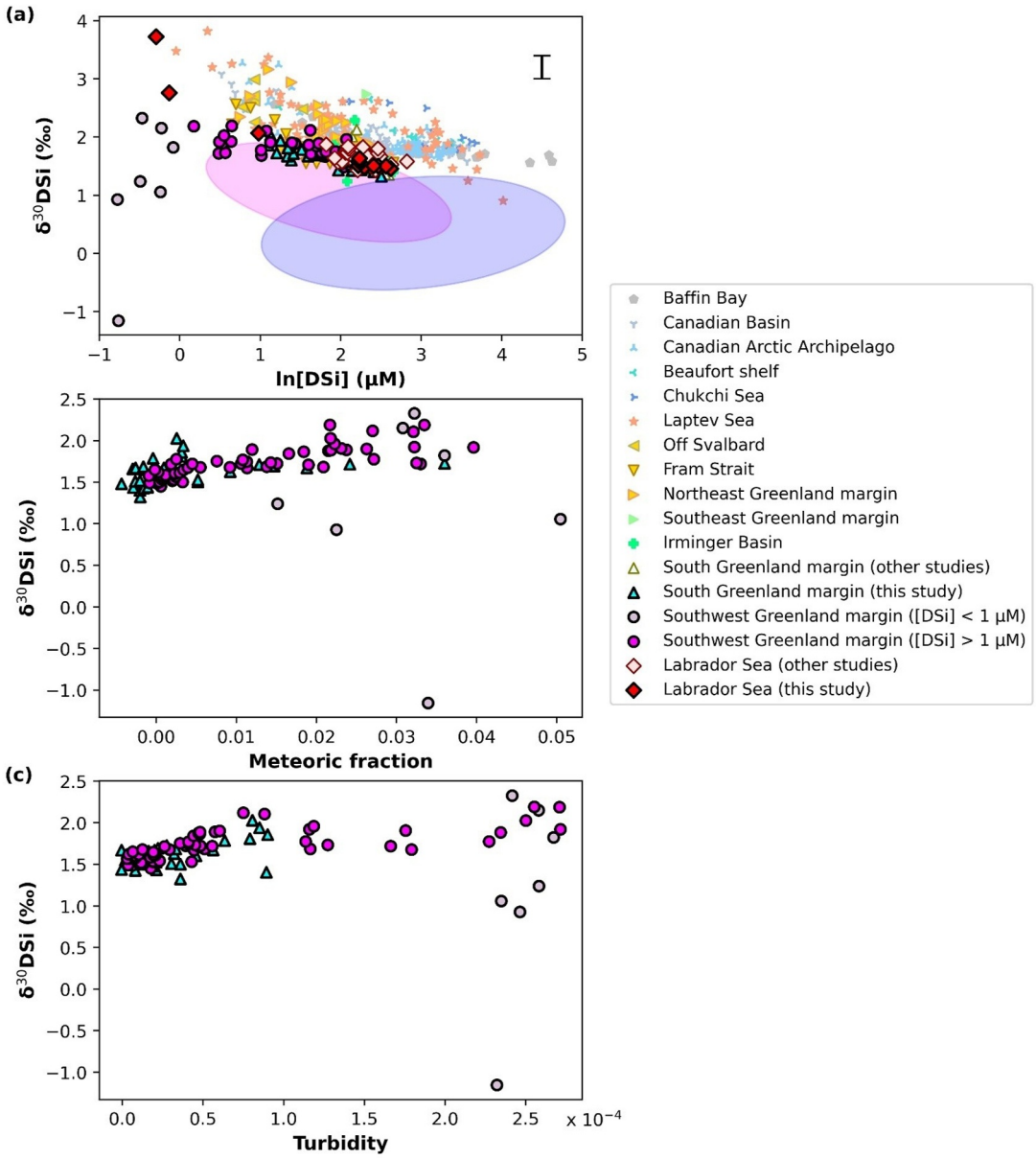

Figure 2. Seawater silicon isotope results and correlation plots. Seawater δ^{30}DSi plotted against (a) the natural logarithm of [DSi]; (b) fraction of meteoric water; and (c) turbidity. Results from this study (emphasized with bold black marker outline) are compared with previously published data from the Arctic Ocean (Table S1 in Supporting Information S1). Error bar shows 2 S.D. of long-term replicate δ^{30}DSi measurements of standards. Magenta and blue ovals represent the range of data from fjords (Hatton et al., 2023) and glacier rivers (Hatton et al., 2019) respectively.

1 to 4 μM (or ln[DSi] from 0 to 1.4 μM, Figure 2a), when compared to those from the other Arctic sites. This near-surface water isotopic difference between our sites and the other Arctic sites is far larger than the known inter-laboratory analytical uncertainties (0.2‰; Grasse et al., 2017).

The plausible explanation for the low apparent fractionation along the southwest margin of Greenland is an additional nutrient source consisting of isotopically-light Si, such as the glacially-sourced ASi that readily dissolves in low [DSi] seawater (Hatton et al., 2019, 2021). Other potential explanations and model artifacts have also been considered and deemed less likely to account for the observation above Supporting Information S1—Low apparent isotopic fractionation, Figure S5 in Supporting Information S1). We have used a simple isotopic model to test that dissolving glacial detritus (ASi) could be a feasible mechanism that reconciles the low apparent fractionation factor in the study area (Supporting Information S1—Isotopic fractionation model). The model

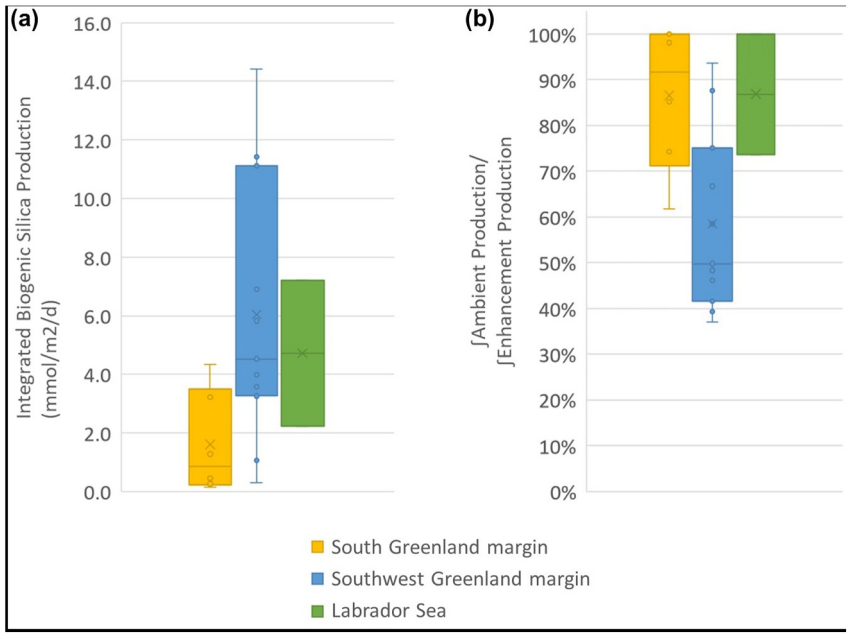

Figure 3. Diatom production results. (a) Summertime diatom BSi production integrated from surface ocean to the base of euphotic zone (defined by 1% isolume). (b) Percentage ratio of depth-integrated diatom production at ambient condition to depth-integrated diatom production at DSi-enhanced (+20 μM) condition. The cross and the horizontal line within each bar indicate the mean and median respectively.

suggests that there are several possible combinations of the following variables: (a) relative contribution of ASi dissolution to the bioavailable Si pool, (b) ASi isotope composition, and (c) the isotopic fractionation factor during diatom uptake that could account for the [DSi]–δ^{30}DSi observations (Figure S6 in Supporting Information S1). These variables will be further assessed in the next section.

Supporting evidence for the notable presence of glacial ASi along the southwest Greenland margin stems from the exceptional standing stock of ASi + BSi relative to [DSi] (Figure 1d) and to Chl *a* (Figure S7a in Supporting Information S1). In fact, the southwest Greenland stations have the second highest [ASi + BSi]/[DSi] observed around the Arctic Ocean (Figure 1d). All these observations suggest a substantial contribution of non-living (detrital) material to the ASi + BSi pool off southwest Greenland. The relative contribution of living diatom BSi and detrital ASi to the ASi + BSi pool can be further estimated from the offset between a computed maximum diatom growth rate at the observed temperature (Kremer et al., 2017) and the measured rate of Si uptake by diatoms (Supporting Information S1—Estimation of detrital contribution to the ASi + BSi pool). The estimation above suggests that up to 87 ± 11% of the ASi + BSi pool off southwest Greenland is detrital, with the remaining portion being living diatoms. The detritus likely contains a significant portion of glacial ASi (and potentially some detrital/dead diatoms) that is transported by modified meltwater, evident from the elevated [ASi + BSi]/[DSi] at higher meteoric fraction (>0.01) among the southwest Greenland stations (Figure S7b in Supporting Information S1).

4.2. Detrital ASi Sustains Coastal Diatom Production

The supply rate of nutrient Si from the dissolving detrital ASi can be further estimated from the detrital ASi composition calculated above and the glacial ASi dissolution rate inferred from previous experiments (Hawkings et al., 2017; Kamatani, 1982) (Supporting Information S1—Estimation of detrital contribution to the ASi + BSi pool). Comparing this estimated nutrient supply rate with the diatom BSi production measured using ^{32}Si tracer suggests that the dissolving detrital ASi could, on average, sustain ~50% of diatom production observed at the Nuuk stations. Considering the inferred ~50% contribution of dissolving detrital ASi to the nutrient pool utilized by diatoms, the isotopic model developed in the previous section suggests that an open system with ASi isotopic composition of +0.8‰ and diatom isotopic fractionation factor of −0.6‰ would best account for the [DSi]–δ^{30}DSi observations at the Nuuk stations (Figure S6 in Supporting Information S1).

The detrital input, most likely containing glacial ASi, may help maintain relatively high levels of diatom production (Figure 3a) on the southwest Greenland margin, and the dissolving detrital ASi can help compensate for lack of BSi dissolution due to low specific rates (driven by the low temperatures) and relatively low DSi in deeper water. Brzezinski et al. (2003) demonstrated that major diatom blooms in many oceanic systems are fueled by "new" sources of Si (akin to new nitrogen in the new production paradigm (Mdutyana et al., 2020)). In many parts of the ocean, such as productive upwelling zones and the Southern Ocean (Tréguer, 2014), such new Si would be largely from deep convective mixing; however, in this region of the Arctic and subarctic, the low DSi:NO_3 ratio of the deep water (Figure S8 in Supporting Information S1) brings proportionally more NO_3 into the euphotic zone than DSi (favoring Si to be exhausted first in a diatom bloom). Thus, our finding suggests that regional diatom blooms can also be sustained by a combination of new Si sources to supplement the low DSi:NO_3 in deeper waters. In addition to glacial ASi, non-glacier rivers have been suggested to be another key source of new Si to the Arctic and subarctic oceans (Holmes et al., 2012; Martin et al., 2020).

Our results indicate that diatoms on the southwest Greenland margin (off Nuuk) experience greater limitation of nutrient DSi (lower $\int\rho_{ambient}/\int\rho_{enhanced}$) than the other study sites (Figure 3b), despite the elevated supply of detrital ASi. Previous studies have shown that certain diatom groups grow much better with the presence of particulates that slowly release silica (Antonella et al., 2003; Grimm et al., 2023). Similarly, the abundance of slowly dissolving detrital ASi particles off southwest Greenland likely has promoted growth of these certain diatom groups with such particulate preference, to the extent that this has caused some degree of nutrient DSi limitation in the area. However, this degree of limitation is well within diatoms' capacity to adapt without affecting their growth rate and is a common observation in marine systems (Krause et al., 2018).

4.3. A Silicon Conveyor Belt

New observations from this study reveal a "conveyor belt" of detrital ASi sourced from fjord, glacial meltwater, and other terrestrial sources, modifying Si cycling off the Greenland coast. Our data provide, for the first time, strong supporting evidence that Si derived from glaciers and potentially other high-latitude fluvial sources are not entirely buried in fjords, but a significant portion can be transported offshore, dominantly in the form of slowly-dissolving ASi, which is utilized by coastal marine primary producers. Despite the slow dissolution of ASi in low temperature seawater, our data show that sufficient accumulation of the dissolving detrital ASi can support a remarkable level of summertime diatom production, despite some degree of nutrient DSi limitation in such low [DSi] seawater.

Glacial erosion contributes disproportionate amounts of suspended sediments that are transported offshore to pan-Arctic coastal regions, particularly around Greenland (Chu et al., 2012; Hasholt et al., 2006). Future climate warming is expected to increase the intensities of (sub)glacial weathering, erosion, and the supply of suspended sediments including ASi to the surrounding oceans (Hatton et al., 2019; Overeem et al., 2017). In the long term, we anticipate large-scale glacier retreat to decrease the transport distance of meltwater and suspended sediments away from the coast, while subsequent exposure of deglaciated watersheds will likely change downstream nutrient transport (Martin et al., 2020). In addition, nutrient supply from other key terrestrial sources, such as the Arctic rivers are also expected to change with climate warming (Terhaar et al., 2021). Complex changes in the supply of nutrient Si from the different sources above, both spatially and temporally (Martin et al., 2020), will likely shift high-latitude hotspots of diatom production over the spring and summer seasons, with important implications for the distribution of higher trophic levels and pan-Arctic economies that utilize these marine resources. Providing quantitative estimates onto the predictions above will require comprehensive modeling that also considers other key regulators of diatom production such as availability of other nutrients and grazing activities.

Conflict of Interest

The authors declare no conflicts of interest relevant to this study.

Data Availability Statement

The article's main new data: (a) seawater dissolved stable silicon isotope (δ^{30}DSi), (b) standing stock of abiogenic and biogenic amorphous solid phases of silica [ASi + BSi], and (c) BSi production (ρ), are available in Pangaea

database, an open data repository which supports the FAIR principles, at Hendry et al. (2024). These data, plus (d) integrated BSi production ($\int\rho$) and (e) the percentage ratio of BSi production at ambient condition to BSi production at DSi-enhanced (+20 μM) condition ($\int\rho_{ambient}/\int\rho_{enhanced}$), are also available in the Data Set S1. Other seawater data collected from the stations, including: potential temperature, salinity, turbidity, chlorophyll a, $\delta^{18}O$, [DSi], and [NO_3] are already available at Hendry (2018).

Acknowledgments
The authors would like to thank the crew, technicians and scientists on RRS Discovery cruise DY081 for all their support. Thanks to Jade Hatton and Christopher Coath for assistance with mass spectrometry. European Research Council ERC starting Grant ICY-LAB 678371 (KRH). Royal Society Grant URF\R \180021 (KRH).

References

Antonella, P., Mauro, M., Ivana, F., Bice, F., Carlo, C., Marco, G., & Bavestrello, G. (2003). Marine diatom growth on different forms of particulate silica: Evidence of cell/particle interaction. *Aquatic Microbial Ecology*, *32*(3), 299–306. https://doi.org/10.3354/ame032299

Arendt, K. E., Nielsen, T. G., Rysgaard, S., & Tönnesson, K. (2010). Differences in plankton community structure along the Godthåbsfjord, from the Greenland Ice Sheet to offshore waters. *Marine Ecology Progress Series*, *401*, 49–62. https://doi.org/10.3354/meps08368

Arrigo, K. R., Dijken, G. L., Castelao, R. M., Luo, H., Rennermalm, Å. K., Tedesco, M., et al. (2017). Melting glaciers stimulate large summer phytoplankton blooms in southwest Greenland waters. *Geophysical Research Letters*, *44*(12), 6278–6285. https://doi.org/10.1002/2017GL073583

Becker, S., Aoyama, M., Woodward, E. M. S., Bakker, K., Coverly, S., Mahaffey, C., & Tanhua, T. (2020). GO-SHIP repeat hydrography nutrient manual: The precise and accurate determination of dissolved inorganic nutrients in seawater, using continuous flow analysis methods. *Frontiers in Marine Science*, *7*, 581790. https://doi.org/10.3389/fmars.2020.581790

Bhatia, M. P., Kujawinski, E. B., Das, S. B., Breier, C. F., Henderson, P. B., & Charette, M. A. (2013). Greenland meltwater as a significant and potentially bioavailable source of iron to the ocean. *Nature Geoscience*, *6*(4), 274–278. https://doi.org/10.1038/ngeo1746

Brzezinski, M. A., Jones, J. L., Bidle, K. D., & Azam, F. (2003). The balance between silica production and silica dissolution in the sea: Insights from Monterey Bay, California, applied to the global data set. *Limnology and Oceanography*, *48*(5), 1846–1854. https://doi.org/10.4319/lo.2003.48.5.1846

Cardinal, D., Alleman, L. Y., de Jong, J., Ziegler, K., & André, L. (2003). Isotopic composition of silicon measured by multicollector plasma source mass spectrometry in dry plasma mode. *Journal of Analytical Atomic Spectrometry*, *18*(3), 213–218. https://doi.org/10.1039/B210109B

Carvalho, F., Kohut, J., Oliver, M. J., & Schofield, O. (2017). Defining the ecologically relevant mixed-layer depth for Antarctica's coastal seas. *Geophysical Research Letters*, *44*(1), 338–345. https://doi.org/10.1002/2016GL071205

Chu, V. W., Smith, L. C., Rennermalm, A. K., Forster, R. R., & Box, J. E. (2012). Hydrologic controls on coastal suspended sediment plumes around the Greenland Ice Sheet. *The Cryosphere*, *6*(1), 1–19. https://doi.org/10.5194/tc-6-1-2012

Debyser, M. C. F., Pichevin, L., Tuerena, R. E., Dodd, P. A., Doncila, A., & Ganeshram, R. S. (2022). Tracing the role of Arctic shelf processes in Si and N cycling and export through the Fram Strait: Insights from combined silicon and nitrate isotopes. *EGUsphere*, *2022*, 1–34. https://doi.org/10.5194/egusphere-2022-254

DeMaster, D. J. (1981). The supply and accumulation of silica in the marine environment. *Geochimica et Cosmochimica Acta*, *45*(10), 1715–1732. https://doi.org/10.1016/0016-7037(81)90006-5

de Souza, G. F., Reynolds, B. C., Rickli, J., Frank, M., Saito, M. A., Gerringa, L. J., & Bourdon, B. (2012). Southern Ocean control of silicon stable isotope distribution in the deep Atlantic Ocean. *Global Biogeochemical Cycles*, *26*(2), GB2035. https://doi.org/10.1029/2011GB004141

Enderlin, E. M., Howat, I. M., Jeong, S., Noh, M.-J., van Angelen, J. H., & van den Broeke, M. R. (2014). An improved mass budget for the Greenland ice sheet. *Geophysical Research Letters*, *41*(3), 866–872. https://doi.org/10.1002/2013GL059010

Felikson, D., Bartholomaus, T. C., Catania, G. A., Korsgaard, N. J., Kjær, K. H., Morlighem, M., et al. (2017). Inland thinning on the Greenland ice sheet controlled by outlet glacier geometry. *Nature Geoscience*, *10*(5), 366–369. https://doi.org/10.1038/ngeo2934

Georg, R. B., Reynolds, B. C., Frank, M., & Halliday, A. N. (2006). New sample preparation techniques for the determination of Si isotopic compositions using MC-ICPMS. *Chemical Geology*, *235*(1), 95–104. https://doi.org/10.1016/j.chemgeo.2006.06.006

Giesbrecht, K. E., & Varela, D. E. (2021). Summertime biogenic silica production and silicon limitation in the Pacific Arctic region from 2006 to 2016. *Global Biogeochemical Cycles*, *35*(1), e2020GB006629. https://doi.org/10.1029/2020GB006629

Giesbrecht, K. E., Varela, D. E., de Souza, G. F., & Maden, C. (2022). Natural variations in dissolved silicon isotopes across the Arctic Ocean from the Pacific to the Atlantic. *Global Biogeochemical Cycles*, *36*(5), e2021GB007107. https://doi.org/10.1029/2021GB007107

Grasse, P., Brzezinski, M. A., Cardinal, D., De Souza, G. F., Andersson, P., Closset, I., et al. (2017). GEOTRACES inter-calibration of the stable silicon isotope composition of dissolved silicic acid in seawater. *Journal of Analytical Atomic Spectrometry*, *32*(3), 562–578. https://doi.org/10.1039/C6JA00302H

Grimm, C., Feurtet-Mazel, A., Pokrovsky, O. S., & Oelkers, E. H. (2023). Riverine Particulate Matter Enhances the Growth and Viability of the Marine Diatom Thalassiosira weissflogii. *Minerals*, *13*(2), 183. https://doi.org/10.3390/min13020183

Hasholt, B., Bobrovitskaya, N., Bogen, J., McNamara, J., Mernild, S., Milburn, D., & Walling, D. E. (2006). Sediment transport to the Arctic Ocean and adjoining cold oceans. *Water Policy*, *37*(4–5), 413–432. https://doi.org/10.2166/nh.2006.023

Hatton, J. E., Hendry, K. R., Hawkings, J. R., Wadham, J. L., Benning, L. G., Blukis, R., et al. (2021). Physical weathering by glaciers enhances silicon mobilisation and isotopic fractionation. *Geochemical Perspectives Letters*, *19*, 7–12. https://doi.org/10.7185/geochemlet.2126

Hatton, J. E., Hendry, K. R., Hawkings, J. R., Wadham, J. L., Kohler, T. J., Stibal, M., et al. (2019). Investigation of subglacial weathering under the Greenland Ice Sheet using silicon isotopes. *Geochimica et Cosmochimica Acta*, *247*, 191–206. https://doi.org/10.1016/j.gca.2018.12.033

Hatton, J. E., Ng, H. C., Meire, L., Woodward, E. M. S., Leng, M. J., Coath, C. D., et al. (2023). Silicon isotopes highlight the role of glaciated fjords in modifying coastal waters. *Journal of Geophysical Research - Biogeosciences*, *128*(7), e2022JG007242. https://doi.org/10.1029/2022JG007242

Hawkings, J. R., Wadham, J. L., Benning, L. G., Hendry, K. R., Tranter, M., Tedstone, A., et al. (2017). Ice sheets as a missing source of silica to the polar oceans. *Nature Communications*, *8*(1), 14198. https://doi.org/10.1038/ncomms14198

Hawkings, J. R., Wadham, J. L., Tranter, M., Raiswell, R., Benning, L. G., Statham, P. J., et al. (2014). Ice sheets as a significant source of highly reactive nanoparticulate iron to the oceans. *Nature Communications*, *5*(1), 3929. https://doi.org/10.1038/ncomms4929

Hendry, K. R. (2018). North Atlantic seawater bottle data collected from CTD during RRS Discovery cruise DY081 [Dataset]. *PANGAEA*. https://doi.org/10.1594/PANGAEA.896543

Hendry, K. R., Briggs, N., Henson, S., Opher, J., Brearley, J. A., Meredith, M. P., et al. (2021). Tracing glacial meltwater from the Greenland Ice Sheet to the ocean using gliders. *Journal of Geophysical Research: Oceans*, *126*(8), e2021JC017274. https://doi.org/10.1029/2021JC017274

Hendry, K. R., Huvenne, V. A. I., Robinson, L. F., Annett, A., Badger, M., Jacobel, A. W., et al. (2019). The biogeochemical impact of glacial meltwater from Southwest Greenland. *Progress in Oceanography*, *176*, 102126. https://doi.org/10.1016/j.pocean.2019.102126

Hendry, K. R., Ng, H. C., & Krause, J. W. (2024). North Atlantic seawater bottle data collected from CTD during RRS Discovery cruise DY081, extended version [Dataset]. *PANGAEA*. https://doi.org/10.1594/PANGAEA.967168

Hendry, K. R., & Robinson, L. F. (2012). The relationship between silicon isotope fractionation in sponges and silicic acid concentration: Modern and core-top studies of biogenic opal. *Geochimica et Cosmochimica Acta*, *81*, 1–12. https://doi.org/10.1016/j.gca.2011.12.010

Holmes, R. M., McClelland, J. W., Peterson, B. J., Tank, S. E., Bulygina, E., Eglinton, T. I., et al. (2012). Seasonal and annual fluxes of nutrients and organic matter from large rivers to the Arctic Ocean and surrounding seas. *Estuaries and Coasts*, *35*(2), 369–382. https://doi.org/10.1007/s12237-011-9386-6

Hopwood, M. J., Bacon, S., Arendt, K., Connelly, D., & Statham, P. (2015). Glacial meltwater from Greenland is not likely to be an important source of Fe to the North Atlantic. *Biogeochemistry*, *124*(1), 1–11. https://doi.org/10.1007/s10533-015-0091-6

Hopwood, M. J., Carroll, D., Dunse, T., Hodson, A., Holding, J. M., Iriarte, J. L., et al. (2020). Review article: How does glacier discharge affect marine biogeochemistry and primary production in the Arctic? *The Cryosphere*, *14*(4), 1347–1383. https://doi.org/10.5194/tc-14-1347-2020

Hughes, H. J., Delvigne, C., Korntheuer, M., de Jong, J., André, L., & Cardinal, D. (2011). Controlling the mass bias introduced by anionic and organic matrices in silicon isotopic measurements by MC-ICP-MS. *Journal of Analytical Atomic Spectrometry*, *26*(9), 1892–1896. https://doi.org/10.1039/C1JA10110B

Hydes, D. J., Aoyama, M., Aminot, A., Bakker, K., Becker, S., Coverly, S., et al. (2010). Recommendations for the determination of nutrients in seawater to high levels of precision and inter-comparability using continuous flow analysers. In *GO-SHIP (Unesco/IOC)*.

Kamatani, A. (1982). Dissolution rates of silica from diatoms decomposing at various temperatures. *Marine Biology*, *68*(1), 91–96. https://doi.org/10.1007/BF00393146

Koziorowska, K., Kuliński, K., & Pempkowiak, J. (2018). Deposition, return flux, and burial rates of nitrogen and phosphorus in the sediments of two high-Arctic fjords. *Oceanologia*, *60*(4), 431–445. https://doi.org/10.1016/j.oceano.2018.05.001

Krause, J. W., Brzezinski, M. A., & Jones, J. L. (2011). Application of low-level beta counting of 32Si for the measurement of silica production rates in aquatic environments. *Marine Chemistry*, *127*(1), 40–47. https://doi.org/10.1016/j.marchem.2011.07.001

Krause, J. W., Duarte, C. M., Marquez, I. A., Assmy, P., Fernández-Méndez, M., Wiedmann, I., et al. (2018). Biogenic silica production and diatom dynamics in the Svalbard region during spring. *Biogeosciences*, *15*(21), 6503–6517. https://doi.org/10.5194/bg-15-6503-2018

Krause, J. W., Schulz, I. K., Rowe, K. A., Dobbins, W., Winding, M. H. S., Sejr, M. K., et al. (2019). Silicic acid limitation drives bloom termination and potential carbon sequestration in an Arctic bloom. *Scientific Reports*, *9*(1), 8149. https://doi.org/10.1038/s41598-019-44587-4

Kremer, C. T., Thomas, M. K., & Litchman, E. (2017). Temperature- and size-scaling of phytoplankton population growth rates: Reconciling the Eppley curve and the metabolic theory of ecology. *Limnology and Oceanography*, *62*(4), 1658–1670. https://doi.org/10.1002/lno.10523

Lam, P. J., Ohnemus, D. C., & Auro, M. E. (2015). Size-fractionated major particle composition and concentrations from the US GEOTRACES North Atlantic zonal transect. *Deep Sea Research Part II: Topical Studies in Oceanography*, *116*, 303–320. https://doi.org/10.1016/j.dsr2.2014.11.020

Laufer-Meiser, K., Michaud, A. B., Maisch, M., Byrne, J. M., Kappler, A., Patterson, M. O., et al. (2021). Potentially bioavailable iron produced through benthic cycling in glaciated Arctic fjords of Svalbard. *Nature Communications*, *12*(1), 1349. https://doi.org/10.1038/s41467-021-21558-w

Laukert, G., Grasse, P., Novikhin, A., Povazhnyi, V., Doering, K., Hölemann, J., et al. (2022). Nutrient and silicon isotope dynamics in the Laptev Sea and implications for nutrient availability in the transpolar drift. *Global Biogeochemical Cycles*, *36*(9), e2022GB007316. https://doi.org/10.1029/2022GB007316

Lewis, K. M., van Dijken, G. L., & Arrigo, K. R. (2020). Changes in phytoplankton concentration now drive increased Arctic Ocean primary production. *Science*, *369*(6500), 198–202. https://doi.org/10.1126/science.aay8380

Martin, J. B., Pain, A. J., Martin, E. E., Rahman, S., & Ackerman, P. (2020). Comparisons of nutrients exported from Greenlandic glacial and deglaciated watersheds. *Global Biogeochemical Cycles*, *34*(12), e2020GB006661. https://doi.org/10.1029/2020GB006661

McNair, H. M., Brzezinski, M. A., & Krause, J. W. (2018). Diatom populations in an upwelling environment decrease silica content to avoid growth limitation. *Environmental Microbiology*, *20*(11), 4184–4193. https://doi.org/10.1111/1462-2920.14431

Mdutyana, M., Thomalla, S. J., Philibert, R., Ward, B. B., & Fawcett, S. E. (2020). The seasonal cycle of nitrogen uptake and Nitrification in the Atlantic sector of the Southern Ocean. *Global Biogeochemical Cycles*, *34*(7), e2019GB006363. https://doi.org/10.1029/2019GB006363

Meire, L., Meire, P., Struyf, E., Krawczyk, D. W., Arendt, K. E., Yde, J. C., et al. (2016). High export of dissolved silica from the Greenland Ice Sheet. *Geophysical Research Letters*, *43*(17), 9173–9182. https://doi.org/10.1002/2016GL070191

Meire, L., Mortensen, J., Meire, P., Juul-Pedersen, T., Sejr, M. K., Rysgaard, S., et al. (2017). Marine-terminating glaciers sustain high productivity in Greenland fjords. *Global Change Biology*, *23*(12), 5344–5357. https://doi.org/10.1111/gcb.13801

Meredith, M., Sommerkorn, M., Cassota, S., Derksen, C., Ekaykin, A., Hollowed, A., et al. (2019). Polar regions.

Nelson, D. M., Tréguer, P., Brzezinski, M. A., Leynaert, A., & Quéguiner, B. (1995). Production and dissolution of biogenic silica in the ocean: Revised global estimates, comparison with regional data and relationship to biogenic sedimentation. *Global Biogeochemical Cycles*, *9*(3), 359–372. https://doi.org/10.1029/95GB01070

Ng, H. C., Cassarino, L., Pickering, R. A., Woodward, E. M. S., Hammond, S. J., & Hendry, K. R. (2020). Sediment efflux of silicon on the Greenland margin and implications for the marine silicon cycle. *Earth and Planetary Science Letters*, *529*, 115877. https://doi.org/10.1016/j.epsl.2019.115877

Ng, H. C., Hawkings, J. R., Bertrand, S., Summers, B. A., Sieber, M., Conway, T. M., et al. (2022). Benthic dissolved silicon and iron cycling at glaciated Patagonian fjord heads. *Global Biogeochemical Cycles*, *36*(11), e2022GB007493. https://doi.org/10.1029/2022GB007493

Oliver, H., Luo, H., Castelao, R. M., van Dijken, G. L., Mattingly, K. S., Rosen, J. J., et al. (2018). Exploring the potential impact of Greenland meltwater on stratification, photosynthetically active radiation, and primary production in the Labrador Sea. *Journal of Geophysical Research: Oceans*, *123*(4), 2570–2591. https://doi.org/10.1002/2018JC013802

Overeem, I., Hudson, B. D., Syvitski, J. P. M., Mikkelsen, A. B., Hasholt, B., van den Broeke, M. R., et al. (2017). Substantial export of suspended sediment to the global oceans from glacial erosion in Greenland. *Nature Geoscience*, *10*(11), 859–863. https://doi.org/10.1038/ngeo3046

Reynolds, B. C., Aggarwal, J., Andre, L., Baxter, D., Beucher, C., Brzezinski, M. A., et al. (2007). An inter-laboratory comparison of Si isotope reference materials. *Journal of Analytical Atomic Spectrometry*, *22*(5), 561–568. https://doi.org/10.1039/B616755A

Rysgaard, S., Boone, W., Carlson, D., Sejr, M. K., Bendtsen, J., Juul-Pedersen, T., et al. (2020). An updated view on water masses on the pan-west Greenland continental shelf and their link to proglacial fjords. *Journal of Geophysical Research: Oceans*, *125*(2), e2019JC015564. https://doi.org/10.1029/2019JC015564

Shepherd, A., Ivins, E., Rignot, E., Smith, B., van den Broeke, M., Velicogna, I., et al. (2020). Mass balance of the Greenland ice sheet from 1992 to 2018. *Nature*, *579*(7798), 233–239. https://doi.org/10.1038/s41586-019-1855-2

Sutton, J. N., Souza, G. F. d., Garcia-Ibiliez, M. I., & De La Rocha, C. L. (2018). The silicon stable isotope distribution along the GEOVIDE section (GEOTRACES GA-01) of the North Atlantic Ocean. *Biogeosciences*, *15*(18), 5663–5676. https://doi.org/10.5194/bg-15-5663-2018

Terhaar, J., Lauerwald, R., Regnier, P., Gruber, N., & Bopp, L. (2021). Around one third of current Arctic Ocean primary production sustained by rivers and coastal erosion. *Nature Communications*, *12*(1), 169. https://doi.org/10.1038/s41467-020-20470-z

Tonnard, M., Planquette, H., Bowie, A. R., van der Merwe, P., Gallinari, M., Desprez de Gésincourt, F., et al. (2020). Dissolved iron in the north Atlantic ocean and Labrador Sea along the GEOVIDE section (GEOTRACES section GA01). *Biogeosciences*, *17*(4), 917–943. https://doi.org/10.5194/bg-17-917-2020

Tréguer, P. J. (2014). The Southern Ocean silica cycle. *Comptes Rendus Geoscience*, *346*(11), 279–286. https://doi.org/10.1016/j.crte.2014.07.003

van den Broeke, M., Box, J., Fettweis, X., Hanna, E., Noël, B., Tedesco, M., et al. (2017). Greenland ice sheet surface mass loss: Recent developments in observation and modeling. *Current Climate Change Reports*, *3*(4), 345–356. https://doi.org/10.1007/s40641-017-0084-8

Varela, D. E., Pride, C. J., & Brzezinski, M. A. (2004). Biological fractionation of silicon isotopes in Southern Ocean surface waters. *Global Biogeochemical Cycles*, *18*(1). https://doi.org/10.1029/2003GB002140

Woodward, E. M. S., & Rees, A. P. (2001). Nutrient distributions in an anticyclonic eddy in the northeast Atlantic Ocean, with reference to nanomolar ammonium concentrations. *Deep Sea Research Part II: Topical Studies in Oceanography*, *48*(4), 775–793. https://doi.org/10.1016/S0967-0645(00)00097-7

References From the Supporting Information

Brzezinski, M. A., & Phillips, D. R. (1997). Evaluation of 32Si as a tracer for measuring silica production rates in marine waters. *Limnology and Oceanography*, *42*(5), 856–865. https://doi.org/10.4319/lo.1997.42.5.0856

Brzezinski, M. A., Closset, I., Jones, J. L., de Souza, G. F., & Maden, C. (2021). New constraints on the physical and biological controls on the silicon isotopic composition of the Arctic Ocean. *Frontiers in Marine Science*, *8*. https://doi.org/10.3389/fmars.2021.699762

de la Rocha, C. L., Brzezinski, M. A., & DeNiro, M. J. (1997). Fractionation of silicon isotopes by marine diatoms during biogenic silica formation. *Geochimica et Cosmochimica Acta*, *61*(23), 5051–5056. https://doi.org/10.1016/S0016-7037(97)00300-1

Demarest, M. S., Brzezinski, M. A., & Beucher, C. P. (2009). Fractionation of silicon isotopes during biogenic silica dissolution. *Geochimica et Cosmochimica Acta*, *73*(19), 5572–5583. https://doi.org/10.1016/j.gca.2009.06.019

Egan, K. E., Rickaby, R. E. M., Leng, M. J., Hendry, K. R., Hermoso, M., Sloane, H. J., et al. (2012). Diatom silicon isotopes as a proxy for silicic acid utilisation: A Southern Ocean core top calibration. *Geochimica et Cosmochimica Acta*, *96*, 174–192. https://doi.org/10.1016/j.gca.2012.08.002

Krause, J. W., Brzezinski, M. A., Landry, M. R., Baines, S. B., Nelson, D. M., Selph, K. E., et al. (2010). The effects of biogenic silica detritus, zooplankton grazing, and diatom size structure on silicon cycling in the euphotic zone of the eastern equatorial Pacific. *Limnology and Oceanography*, *55*(6), 2608–2622. https://doi.org/10.4319/lo.2010.55.6.2608

Lund-Hansen, L. C., Andersen, T. J., Nielsen, M. H., & Pejrup, M. (2010). Suspended matter, Chl-a, CDOM, Grain sizes, and optical properties in the Arctic fjord-Type estuary, Kangerlussuaq, West Greenland During summer. *Estuaries and Coasts*, *33*(6), 1442–1451. https://doi.org/10.1007/s12237-010-9300-7

Lund Paulsen, M., Müller, O., Larsen, A., Møller, E. F., Middelboe, M., Sejr, M. K., & Stedmon, C. (2019). Biological transformation of Arctic dissolved organic matter in a NE Greenland fjord. *Limnology and Oceanography*, *64*(3), 1014–1033. https://doi.org/10.1002/lno.11091

Mortensen, J., Rysgaard, S., Winding, M. H. S., Juul-Pedersen, T., Arendt, K. E., Lund, H., et al. (2022). Multidecadal water mass dynamics on the West Greenland shelf. *Journal of Geophysical Research: Oceans*, *127*(7), e2022JC018724. https://doi.org/10.1029/2022JC018724

Murray, C., Markager, S., Stedmon, C. A., Juul-Pedersen, T., Sejr, M. K., & Bruhn, A. (2015). The influence of glacial melt water on bio-optical properties in two contrasting Greenlandic fjords. *Estuarine, Coastal and Shelf Science*, *163*, 72–83. https://doi.org/10.1016/j.ecss.2015.05.041

NOAA. (2009). *ETOPO1 1 Arc-Minute global Relief model*. NOAA National Centers for Environmental Information. https://doi.org/10.7289/V5C8276M

Pickering, R. A., Cassarino, L., Hendry, K. R., Wang, X. L., Maiti, K., & Krause, J. W. (2020). Using stable isotopes to disentangle marine sedimentary signals in reactive silicon pools. *Geophysical Research Letters*, *47*(15), e2020GL087877. https://doi.org/10.1029/2020GL087877

Raiswell, R., Tranter, M., Benning, L. G., Siegert, M., De'ath, R., Huybrechts, P., & Payne, T. (2006). Contributions from glacially derived sediment to the global iron (oxyhydr)oxide cycle: Implications for iron delivery to the oceans. *Geochimica et Cosmochimica Acta*, *70*(11), 2765–2780. https://doi.org/10.1016/j.gca.2005.12.027

Schlitzer, R. (2012). Ocean data view. Retrieved from http://odv.awi.de/

Shoenfelt, E. M., Winckler, G., Annett, A. L., Hendry, K. R., & Bostick, B. C. (2019). Physical weathering intensity controls bioavailable primary iron(II) silicate content in major global dust sources. *Geophysical Research Letters*, *46*(19), 10854–10864. https://doi.org/10.1029/2019GL084180

Stamm, F. M., Méheut, M., Zambardi, T., Chmeleff, J., Schott, J., & Oelkers, E. H. (2020). Extreme silicon isotope fractionation due to Si organic complexation: Implications for silica biomineralization. *Earth and Planetary Science Letters*, *541*, 116287. https://doi.org/10.1016/j.epsl.2020.116287

Sutton, J. N., Varela, D. E., Brzezinski, M. A., & Beucher, C. P. (2013). Species-dependent silicon isotope fractionation by marine diatoms. *Geochimica et Cosmochimica Acta*, *104*, 300–309. https://doi.org/10.1016/j.gca.2012.10.057

Varela, D. E., Brzezinski, M. A., Beucher, C. P., Jones, J. L., Giesbrecht, K. E., Lansard, B., & Mucci, A. (2016). Heavy silicon isotopic composition of silicic acid and biogenic silica in Arctic waters over the Beaufort shelf and the Canada Basin. *Global Biogeochemical Cycles*, *30*(6), 804–824. https://doi.org/10.1002/2015gb005277

Ward, J. P. J., Hendry, K. R., Arndt, S., Faust, J. C., Freitas, F. S., Henley, S. F., et al. (2022). Benthic silicon cycling in the Arctic Barents sea: A reaction-transport model study. *Biogeosciences*, *19*(14), 3445–3467. https://doi.org/10.5194/bg-19-3445-2022

Wetzel, F., de Souza, G. F., & Reynolds, B. C. (2014). What controls silicon isotope fractionation during dissolution of diatom opal? *Geochimica et Cosmochimica Acta*, *131*, 128–137. https://doi.org/10.1016/j.gca.2014.01.028